

Real time monitoring of polymerization rate of methyl methacrylate using fluorescence probe

Ö. Pekcan* and Y. Yılmaz

Istanbul Technical University, Department of Physics, Maslak, 80626 Istanbul, Turkey

and O. Okay

TUBITAK Marmara Research Center and Kocaeli University, Department of Chemistry, PO Box 21, 41470 Gebze, Kocaeli, Turkey

(Received 19 March 1996; revised 14 May 1996)

The steady-state fluorescence technique was used to study the polymerization rate and the autoacceleration due to the gel effect in free-radical polymerization of methyl methacrylate. Pyrene was used as a fluorescence probe for the *in situ* polymerization experiments. The times required for the onset of the gel effect were recorded for various polymerization temperatures. A simple kinetic model was used to validate the experimental data. The results show that the fluorescence technique can be used to follow the onset of the gel effect and the activation energy during the polymerization processes. © 1997 Elsevier Science Ltd. All rights reserved.

(Keywords: steady-state fluorescence technique; free-radical polymerization; gel effect)

INTRODUCTION

Steady-state fluorescence spectra of many chromophores are sensitive to the polarity of their environment. The interactions between the chromophore and the solvent molecules affect the energy difference between the ground and the excited states. This energy difference is called the Stokes shift, and depends on the refractive index and dielectric constant of the solvent. Recently, by measuring the Stokes shift of a polarity sensitive fluorescence molecule, the gelation during epoxy curing was monitored as a function of cure time¹. Time-resolved and steady-state fluorescence techniques were employed to study isotactic polystyrene in its gel state. Excimer spectra were used to monitor the existence of two different conformations in the gel state of polystyrene. A pyrene (Py) derivative was used as a fluorescence molecule to monitor the polymerization, ageing and drying of aluminosilicate gels. These results were interpreted in terms of the chemical changes occurring during the sol–gel process and the interactions between the chromophores and the sol–gel matrix. Recently, we reported *in situ* observations of the sol–gel phase transition in free-radical crosslinking copolymerization using the fluorescence technique^{2–4}.

The gel effect, also called the Trommsdorf effect in free-radical polymerization of vinyl monomers, is a well known phenomenon that is accompanied by an increase in both rate and degree of polymerization^{5–7}. Methyl methacrylate (MMA) polymerization in bulk also shows a very pronounced gel effect caused by diffusion control

of the termination reaction⁸. This is a result of increased viscosity of the reaction solution of poly(methyl methacrylate) (PMMA) in MMA monomer. Thus, during the free-radical polymerization of MMA the monomer conversion first increases only slightly, but then it accelerates due to the gel effect. In this paper we use the quenching properties of the excited state of a fluorescing molecule to study the gel effect in free-radical polymerization of MMA. Py is used as a fluorescence probe for the *in situ* polymerization experiments. The rate of polymerization and the time required for the onset of the gel effect were determined at various temperatures, and the activation energy for the gel effect was also calculated. In order to interpret the data a kinetic model is used which combines concepts given in the literature⁹.

THEORETICAL CONSIDERATIONS

Fluorescence method

Fluorescence and phosphorescence intensities of aromatic molecules are affected by both radiative and non-radiative processes¹⁰. If the possibility of perturbation due to oxygen is excluded, the radiative probabilities are found to be relatively independent of the environment and even of molecular species. Environmental effects on non-radiative transitions, which are primarily intramolecular in nature, are believed to arise from a breakdown of the Born–Oppenheimer approximation¹¹. The role of the solvent in such a picture is to add the quasi-continuum of states needed to satisfy energy resonance conditions. The solvent acts as an energy sink for rapid vibrational relaxation, which occurs after the rate limiting transition from the initial state.

* To whom correspondence should be addressed

Years ago, Birks *et al.* studied the influence of solvent viscosity on fluorescence characteristics of Py solutions in various solvents and observed that the rate of monomer internal quenching is affected by solvent quality¹². Kamioka *et al.* reported the solvent dependence of energy trapping in phenanthrene block polymers and explained the decrease in fluorescence yield with the static quenching, caused by the solvent induced trapping states¹³. As the temperature of the liquid solution is varied, the environment about the molecule changes and much of the change in absorption spectra and fluorescence yields in solution can be related to the changes in solvent viscosity. A matrix that changes little with temperature will enable one to study molecular properties themselves without changing environmental influence. PMMA has been used as such a matrix in many studies¹⁴. Recently we have reported viscosity effects on low frequency, intramolecular vibrational energies of excited naphthalene in swollen PMMA latex particles¹⁵.

Rate of polymerization

The change of monomer conversion χ with the reaction time t for an isothermal polymerization can be written as follows¹⁶:

$$\frac{dx}{dt} = k_p[R\cdot](1 - \chi) \tag{1}$$

where $[R\cdot]$ is the steady-state concentration of the radicals, which can be expressed as

$$[R\cdot] = \left(\frac{2fk_d[I]}{k_t}\right)^{1/2} \tag{1a}$$

k_p and k_t are the rate constants for propagation and termination respectively, and k_d is the decomposition rate constant of the initiator I whose concentration is given by⁸

$$\frac{d[I]}{dt} = k_d[I] - \frac{\epsilon}{1 + \epsilon x} [I] \frac{d\chi}{dt}$$

where f is the initiator efficiency, and ϵ is the contraction factor. Experimental observations indicate that in free-radical polymerization the propagation and chain transfer reactions as well as the initiator efficiency are diffusion limited especially at high conversions. Moreover, bimolecular termination reactions are also diffusion controlled, even at zero monomer conversion. Therefore, the rate constants k_p and k_t as well as f in equations (1) and (1a) are actually not constant, but a function of the conversion x . The variation of these parameters with conversion will be explained in the next section.

The instantaneous number and weight average molecular weights in free-radical polymerization, M_n and M_w , respectively, are

$$M_n = M_m \frac{2}{2\tau + \beta} \tag{3}$$

$$M_w = M_m \frac{2\tau + 3\beta}{(\tau + \beta)^2} \tag{4}$$

where $\tau = \lambda k_t[R\cdot] + k_{tr,M}[M]/k_p[M]$, $\beta = (1 - \lambda)k_t[R\cdot]/k_p[M]$, $[M]$ is the monomer concentration, i.e. $[M] = 1000\rho_M(1 - x)/M_m(1 + \epsilon x)$, M_m and ρ_M are the

molecular weight and the density of the monomer MMA, λ is the fraction of radicals participating in disproportionation termination, and $k_{tr,M}$ is the rate constant for the chain transfer reactions to the monomer. The cumulative molecular weights are obtained as follows:

$$\frac{d\bar{M}_n}{dt} = \frac{\bar{M}_n \left(1 - \frac{\bar{M}_n}{M_n}\right)}{x} \frac{dx}{dt} \tag{5}$$

$$\frac{d\bar{M}_w}{dt} = \frac{M_w - \bar{M}_w}{x} \frac{dx}{dt} \tag{6}$$

Diffusion control

If the rate of a reaction between two species in a solvent cage is much less than their diffusion rate towards each other through the solvent, then the reaction is said to be chemically controlled. In the case of diffusion-controlled reactions, the rate of diffusion of the reactants toward each other is much less than the reaction rate in a solvent cage. Thus, the reaction rate is dependent on the diffusion rates of the reactants. The majority of the fundamental kinetic processes of polymerization belong to this category so that the diffusion control is operative¹⁷. Many theoretical models describing the diffusion controlled processes have been proposed. For the present study, we will use a model proposed recently by Panke for free-radical polymerization of MMA⁹. This model combines the advantages of two models proposed by Hamielec and co-workers^{18,19} and by Buback²⁰⁻²². According to this model, the overall propagation rate constant k_p and the rate constant for the chain transfer reactions to the monomer $k_{tr,M}$ are given as follows:

$$k_p = \frac{1}{\exp\left[\nu_p^* \left(\frac{1}{\nu_f} - \frac{1}{\nu_f^0}\right)\right] \left(\frac{1}{k_p^0} - \frac{1}{k_{p,d}^0} + \frac{1}{k_{p,d}^0}\right)} \tag{7}$$

$$k_{tr,M} = \frac{1}{\exp\left[\nu_p^* \left(\frac{1}{\nu_f} - \frac{1}{\nu_f^0}\right)\right] \left(\frac{1}{k_{tr,M}^0} - \frac{1}{k_{p,d}^0} + \frac{1}{k_{p,d}^0}\right)} \tag{8}$$

Here, k_p^0 and $k_{tr,M}^0$ are the values of k_p and $k_{tr,M}$, respectively, at zero monomer conversion, $k_{p,d}^0$ and ν_p^* are adjustable parameters, ν_f is the actual free volume, and ν_f^0 is the free volume at zero monomer conversion. The free volume of the polymerization system is given by

$$\nu_f = 0.025 + \Delta\alpha_p(T - T_{gp}) \frac{x(1 + \epsilon)}{(1 + \epsilon x)} + \Delta\alpha_M(T - T_{gM}) \frac{(1 - x)}{(1 + \epsilon x)} \tag{9}$$

where $\Delta\alpha_p$ and $\Delta\alpha_M$ are the differences of the expansion coefficients for the liquid and the glassy state for the polymer and monomer, respectively, T_{gp} and T_{gM} are the corresponding glass transition temperatures, and T is the polymerization temperature.

The initiator efficiency f is also diffusion controlled and it starts to decrease at high conversions; f is given by

the following equation⁹:

$$f = \frac{1}{1 + \left(\frac{1}{f^0} - 1\right) \exp\left[\nu_p^* \left(\frac{1}{\nu_f} - \frac{1}{\nu_f^0}\right)\right]} \quad (10)$$

where f^0 is the initiator efficiency at low conversions.

It is usual to distinguish two diffusion steps in the termination process: (a) the translational diffusion of the centre of mass of the polymer molecules towards each other through the solvent, and (b) segmental diffusion of the two chain ends to encounter each other. This occurs by translational and rotational diffusion of those segments bearing active chain ends, or by micro-Brownian motion of segments. In free-radical polymerization, segmental diffusion controls termination rates at low conversions whereas translational diffusion dominates at high conversions. In addition to translational and segmental diffusion control, the termination process is dominated for highly entangled or crosslinked polymeric radicals, i.e. at higher degrees of conversion by reaction diffusion ('propagation diffusion' or 'residual termination'). According to the model proposed by Panke⁹, the following equation can be written for the termination rate constant k_t :

$$k_t = \left[\frac{1}{k_t^0 - C_{RD} k_p^0 [M]^0} - \frac{(\overline{M}_w^0)^{2n}}{k'_{TD}} + \frac{(M_w \overline{M}_w)^n \exp\left[\nu_t^* \left(\frac{1}{\nu_f} - \frac{1}{\nu_f^0}\right)\right]}{k'_{TD}} \right]^{-1} + C_{RD} k_p [M] \quad (11)$$

where the superscript '0' denotes the values at zero monomer conversion, C_{RD} , is the reaction diffusion parameter, and k'_{TD} , ν_t^* and n are adjustable model parameters.

Equations (1)–(11) of the kinetic model can be solved simultaneously to evaluate the monomer conversions, molecular weight averages and the rate constants as a function of the reaction time. Recently Panke used 65

time-conversion curves for the bulk polymerization of MMA in the presence of 2,2'-azobisisobutyronitrile (AIBN) as an initiator to evaluate all the necessary kinetic constants⁹. These constants are collected in Table 1 and will be used to evaluate the experimental data of the present work.

EXPERIMENTAL

In this work we monitored the free-radical polymerization (FRP) of MMA by using an *in situ* steady-state fluorescence technique. The FRP processes were performed separately at 65, 70, 75, 80 and 85°C and monitored against reaction time t . The radical polymerization of MMA was performed in bulk in the presence of AIBN as an initiator. The monomer MMA (Merck) was freed from the inhibitor by shaking with a 10% aqueous KOH, washing with water and drying over sodium sulfate. It was then distilled under reduced pressure over copper chloride. The initiator, AIBN (Merck), was recrystallized twice from methanol. Py was used as a fluorescence probe to detect the FRP process, where MMA and linear PMMA chains act as an energy sink for the excited Py during polymerization. Later, the formation of bulk PMMA provides an ideal, unchanged environment for the excited Py molecules. Naturally, from these experiments one may expect a substantial increase in the fluorescence intensity, I , of Py at a certain time interval, i.e. at the onset of the gel effect.

AIBN (0.26 wt%) was dissolved in MMA and this stock solution was divided and transferred into round glass tubes of 15 mm internal diameter for fluorescence measurements. Six different samples were prepared for the fluorescence experiments. All samples were deoxygenated by bubbling nitrogen for 10 min and then radical polymerization of MMA was performed in the fluorescence accessory of spectrometer. The Py molecule was excited at 345 nm during *in situ* experiments, and the variation in fluorescence emission intensity, I , was monitored with the time-drive mode of the spectrometer, by staying at the 395 nm peak of the Py spectra. *In situ* steady-state fluorescence measurements were carried out

Table 1 Kinetic parameters used in the calculations⁹

Constant	Reference
$k_p^0 = 4.77 \times 10^7 \text{ (1 mol}^{-1} \text{ s}^{-1}) \{ \exp[-31.29 \text{ kJ}/(RT)] \}$	8
$k_t^0 = 6.58 \times 10^{10} \text{ (1 mol}^{-1} \text{ s}^{-1}) \{ \exp[-21.10 \text{ kJ}/(RT)] \}$	8
$k_{tr,M}^0 = 3.54 \times 10^6 \text{ (1 mol}^{-1} \text{ s}^{-1}) \{ \exp[-55.05 \text{ kJ}/(RT)] \}$	22
$k_d = 5.88 \times 10^{15} \text{ s}^{-1} \{ \exp[-133.0 \text{ kJ}/(RT)] \}$	8
$\lambda = 34.81 \text{ (exp}[-12.14 \text{ kJ}/(RT)] \}$	23
$C_{RD} = 1.1171 \text{ mol}^{-1}$	21
$-\epsilon = 0.2256 + 4.81 \times 10^{-4}(T - 273) + 4.1 \times 10^{-7}(T - 273)^2$	8
$\rho_M = 0.9659 - 1.2129 \times 10^{-4}(T - 273) + 1.6816 \times 10^{-6}(T - 273)^2 - 1.0164 \times 10^{-8}(T - 273)^3$	8
$T_{gp} = 114^\circ\text{C}; \quad T_{gm} = -106^\circ\text{C}$	24
$\Delta\alpha_p = 4.8 \times 10^{-4} \text{ K}^{-1}; \quad \Delta\alpha_M = 10^{-3} \text{ K}^{-1}$	24
$f^0 = 6.37 \times 10^{-2} \{ \exp(730.2/T) \}$	9
$k_{pd}^0 = 3.350 \times 10^5 \text{ 1 mol}^{-1} \text{ s}^{-1}$	9
$\nu_p^* = 0.3599$	9
$k'_{TD} = 6.884 \times 10^{13} \text{ 1 mol}^{-1} \text{ s}^{-1}$	9
$\nu_t^* = 1.658$	9
$n = 0.5$	9

using the Model LS-50 spectrometer of Perkin Elmer, equipped with a temperature controller. All measurements were made at the 90° position and slit widths were kept at 2.5 mm.

RESULTS AND DISCUSSION

Typical Py spectra are shown in Figure 1 before and after the onset of the gel effect. No shift was observed in the wavelength of the maximum intensity of Py and all

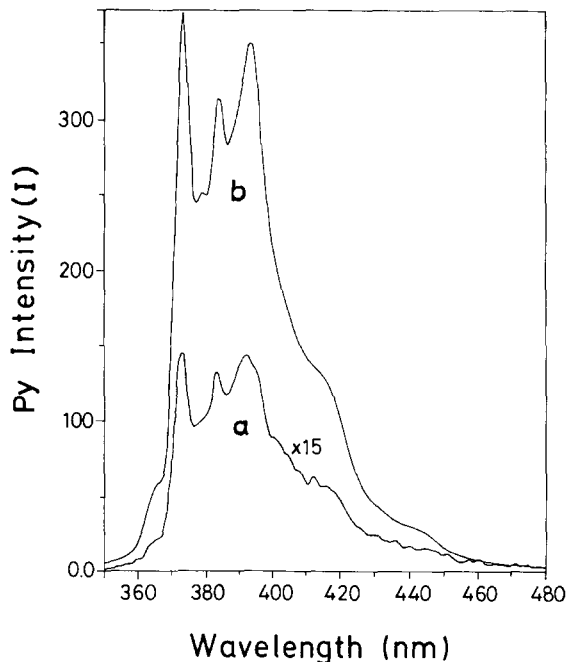


Figure 1 A typical fluorescence emission spectrum of Py (a) before and (b) after the onset of the gel effect in bulk free-radical polymerization (FRP) of MMA in the presence of AIBN (0.26 wt%). Py molecules are excited at 345 nm. Curve (a) was obtained by multiplying the measured curve at 15, i.e. the actual spectrum of Py before the onset of the gel effect is 15 times less intense than the curve (a)

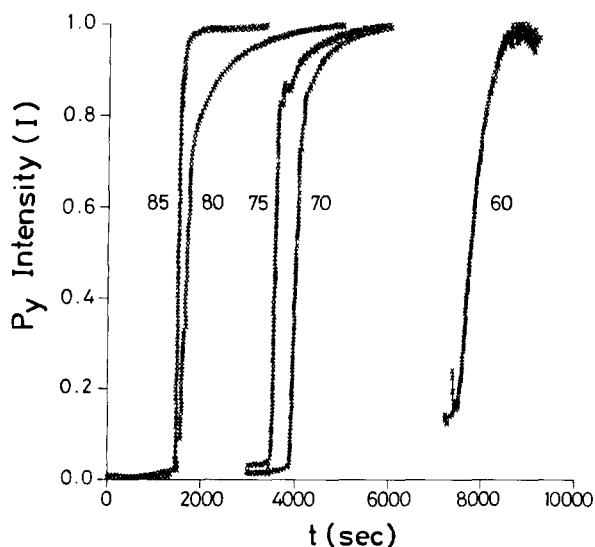


Figure 2 Plots of Py fluorescence intensity *I* versus reaction time *t* during FRP of MMA in bulk and in the presence of AIBN (0.26 wt%). Time-drive mode of the spectrometer was employed and the maximum intensity peak at 395 nm was monitored for data collection. Numbers above the curves indicate the polymerization temperatures in °C

samples kept their transparency during the polymerization process. Scattering light from the samples was also monitored during polymerization experiments and no serious variation was detected at 345 nm intensity. Normalized Py intensities, *I*, versus reaction times are plotted in Figure 2 for samples polymerized at elevated temperatures. In Figure 2, it is seen that all curves present a sudden increase at a given temperature and then reach an equilibrium at later times.

In order to quantify the above results, we assumed that the Py intensity, *I*, increases as polymerization propagates. In order words, as monomer consumption increases due to the polymerization, Py molecules are starting to be trapped in the rigid PMMA environment; as a result *I* increases. Let *t_r* be the time needed for the onset of the gel effect. Below *t_r*, since Py molecules are relatively free, they can interact and be quenched by other molecules; as a result, *I* presents small values. However, above *t_r*, since the reaction mixture is highly viscous, *I* gives very large values. According to Figure 2, at low temperatures the increase in *I* takes place at longer times, indicating that the onset of the gel effect is delayed at low temperatures.

In the following paragraphs it will be shown that *t_r* satisfies the following relation:

$$t_r^{-1} = t_{r0}^{-1} \exp(\Delta E/kT) \tag{12}$$

where *t_{r0}* is a constant, Δ*E* is the activation energy for *t_r* and *k* is the Boltzmann constant. In equation (12), *t_r* is chosen so that the condition *d*²*I/dt*² = 0 is satisfied at *t* = *t_r*. Thus, *t_r* can be determined by taking the first derivative of the experimentally obtained *I* curve with respect to *t*. Figures 3a and b present a typical intensity

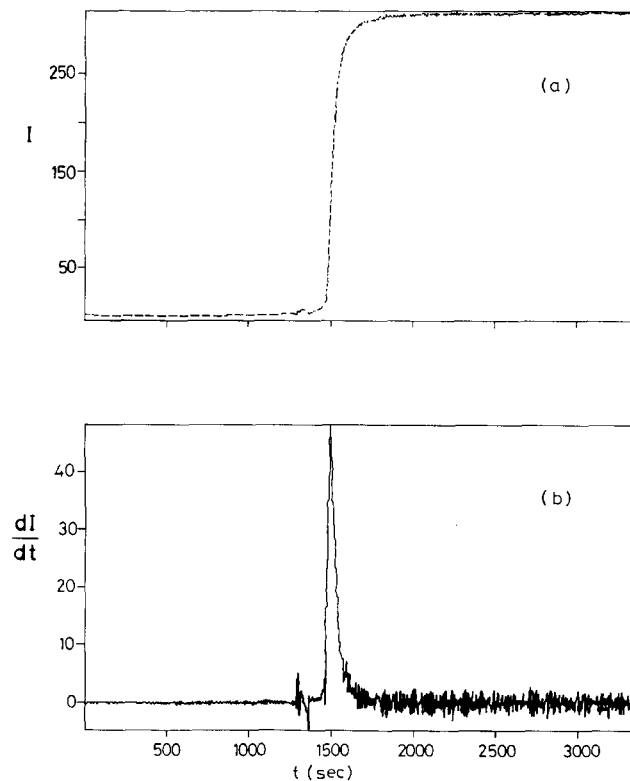


Figure 3 Determination of *t_r* at 80°C: (a) plot of Py fluorescence intensity *I*; (b) its first derivative *dI/dt* versus the reaction time *t*. The maximum corresponds to *t_r* on the *t* axis

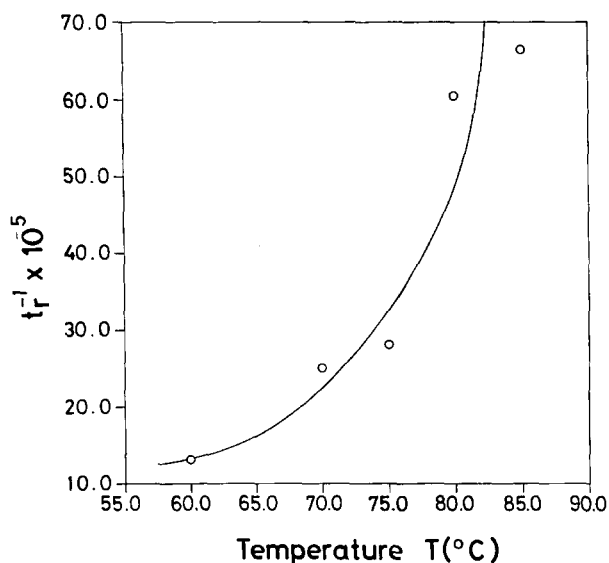


Figure 4 Plot of t_r^{-1} versus temperature T for the samples polymerized at 60, 70, 75, 80 and 85°C

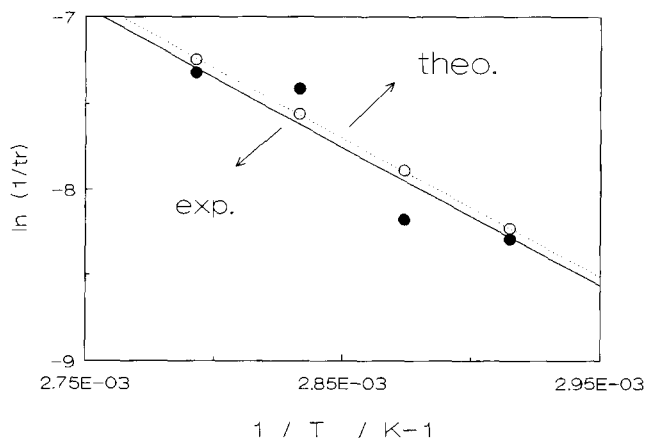


Figure 5 Logarithmic plot of t_r^{-1} versus T^{-1} for the samples polymerized at 60, 70, 75, 80 and 85°C. Experimental data points and calculation results are shown as filled and empty symbols, respectively. The activation energy ΔE produced from the slope of the best fitting lines is $16.1 \text{ kcal mol}^{-1}$

curve and its first derivative (dI/dt) against t , respectively. The maximum in dI/dt curve corresponds to $d^2I/dt^2 = 0$, i.e. to the inflection point in curve I, which gives the t_r , on the time axis. The t_r^{-1} values obtained are plotted versus temperature in Figure 4. As predicted, t_r^{-1} values increase as the temperature is increased. An Arrhenius plot for t_r^{-1} is shown in Figure 5 from which we obtain a good linear relationship (solid line). From the slope of the straight line the activation energy ΔE is obtained as $-16.1 \text{ kcal mol}^{-1}$.

In order to compare the experimental data with the predictions of the kinetic model the parameters collected in ref.9, and also listed in Table 1, were used. The model equations were solved numerically using the Runge-Kutta method. Calculation results for the monomer conversions χ and for the cumulative weight average molecular weights \bar{M}_w are shown in Figures 6a and b, respectively, plotted as a function of the reaction time t for different polymerization temperatures. It is seen that

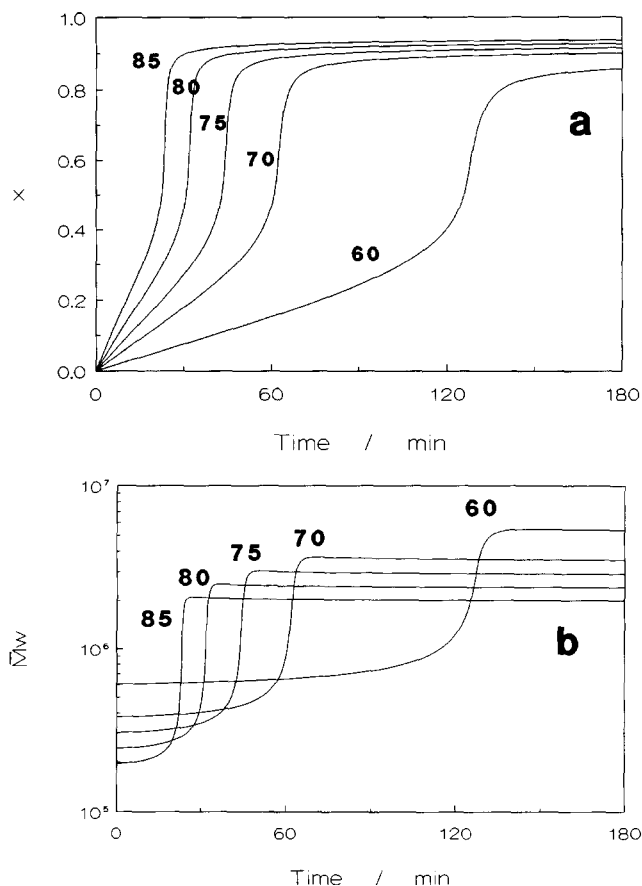


Figure 6 Variation of (a) monomer conversion χ and (b) cumulative weight average molecular weight \bar{M}_w with the reaction time t in FRP of MMA in bulk at different temperatures. The initial concentration of AIBN is 0.018 M (0.26 wt%). The calculations were with use of the kinetic model and with the parameters listed in Table 1. Numbers above the curves indicate the polymerization temperatures in °C

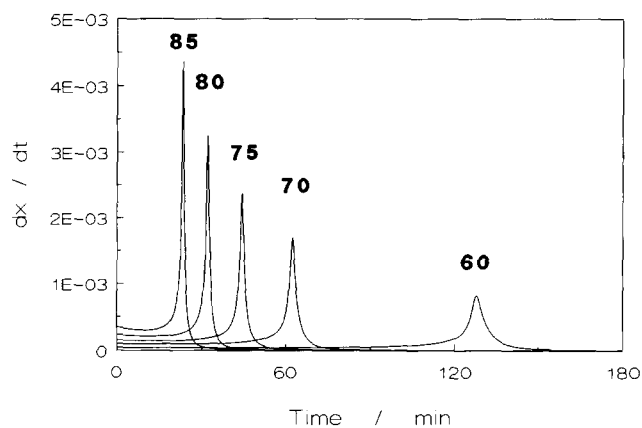


Figure 7 Rate of polymerization of MMA in s^{-1} plotted as a function of the reaction time for different temperatures. Numbers above the curves indicate the polymerization temperatures in °C. The maxima of the curves give the theoretical t_r values from which the theoretical line in Figure 5 was derived

the onset of the gel effect is accompanied by an abrupt increase of monomer conversion and of molecular weight of the polymers, which results in the sudden increase of the Py intensities. In Figure 7, the calculated rates of polymerization for different temperatures are

plotted as a function of the reaction time. The maxima of these curves correspond to the inflection points in χ versus t curves with t_r values on the time axes. The t_r values were evaluated for different temperatures, and the corresponding Arrhenius plot is shown in Figure 5 as the dotted line. Here, the filled and empty symbols represent the experimental and theoretical $\ln(t_r^{-1})$ values, respectively. Excellent agreement between theory and experiment can be seen from the figure. From the slope of the dotted line the theoretical activation energy is calculated as $\Delta E = -16.1 \text{ kcal mol}^{-1}$, which is the value found using fluorescence measurements.

In conclusion, this work introduced a novel fluorescence technique to measure the rate of polymerization, the onset of the gel effect and the corresponding activation energy. Comparison with a kinetic model shows that this simple novel technique is really appropriate for measuring polymerization parameters.

REFERENCES

- 1 Panxviel, J. C., Dunn, B. and Zink, J. J. *J. Phys. Chem.* 1994, **93**, 2134
- 2 Pekcan, Ö, Yilmaz, Y. and Okay, O. *Chem. Phys. Lett.* 1994, **229**, 537
- 3 Pekcan, Ö, Yilmaz, Y. and Okay, O. *Polymer* 1995, **37**, 2049
- 4 Pekcan, Ö, Yilmaz, Y. and Okay, O. *J. Appl. Polym. Sci.* (in press)
- 5 Mahabadi, H. K. and O'Driscoll, K. F. *J. Polym. Sci., Polym. Chem. Edn* 1977, **15**, 283
- 6 Dionisio, J., Mahabadi, H. K. and O'Driscoll, K. F. *J. Polym. Sci.: Polym. Chem. Edn* 1979, **17**, 1891
- 7 Maxwell, I. A. and Russell, G. T. *Macromol. Theory Simul.* 1993, **2**, 95
- 8 Panke, D., Stickler, M. and Wunderlich, W. *Makromol. Chem.* 1983, **184**, 175
- 9 Panke, D. *Macromol. Theory Simul.* 1995, **4**, 759
- 10 Kropp, L. J. and Dawson, R. W. in 'International Conference on Molecular Luminescence' (Ed. E. C. Lim), Benjamin, New York, 1969
- 11 Bixon, M. and Jortner, J. *J. Chem. Phys.* 1968, **48**, 715
- 12 Birks, J. B., Lumb, M. D. and Munro, I. H. *Proc. Roy. Soc. A* 1964, **277**, 289
- 13 Kamioka, K., Weber, S. E. and Morishima, Y. *Macromolecules* 1988, **21**, 972
- 14 Jones, P. F. and Siegel, S. *J. Chem. Phys.* 1969, **50**, 1134
- 15 Pekcan, Ö. *J. Appl. Polym. Sci.* 1995, **57**, 25
- 16 Young, R. J. 'Introduction to Polymers', Chapman and Hall, New York, 1983
- 17 Mita, I. and Horie, K. *J. Macromol. Chem. Phys. C* 1987, **27**, 91
- 18 Marten, F. L. and Hamielec, A. E. in 'Polymerization Reactors and Processes' (Eds J. H. Henderson and T. C. Bouton), ACS Symposium Series 104, American Chemical Society, Washington, DC, 1979
- 19 Stickler, M., Panke, D. and Hamielec, A. E. *J. Polym. Sci.: Polym. Chem. Edn* 1984, **22**, 2243
- 20 Buback, M. *Makromol. Chem.* 1990, **191**, 1575
- 21 Stickler, M. *Makromol. Chem.* 1983, **184**, 2563
- 22 Stickler, M. and Meyerhoff, G. *Makromol. Chem.* 1978, **179**, 2729